Title

Temporal Stability and Prognostic Biomarker Potential of the Prostate Cancer Urine miRNA Transcriptome

Journal

Journal of the National Cancer Institute, 112(3)

ISSN

0027-8874

Authors

Jeon, Jouhyun
Olkhov-Mitsel, Ekaterina
Xie, Honglei
et al.

Publication Date

2020-03-01

DOI

10.1093/jnci/djz112

Peer reviewed

OXFORD

JNCI J Natl Cancer Inst (2020) 112(3): djz112

doi: 10.1093/jnci/djz112
First published online June 4, 2019
Article

ARTICLE

Temporal Stability and Prognostic Biomarker Potential of the Prostate Cancer Urine miRNA Transcriptome

Jouhyun Jeon, Ekaterina Olkhov-Mitsel, Honglei Xie, Cindy Q. Yao, Fang Zhao, Sahar Jahangiri, Carmelle Cuizon, Seville Scarcello, Renu Jeyapala, John D. Watson, Michael Fraser, Jessica Ray, Kristina Commisso, Andrew Loblaw, Neil E. Fleshner, Robert G. Bristow, Michelle Downes, Danny Vesprini, Stanley Liu, Bharati Bapat, Paul C. Boutros

See the Notes section for the full list of authors' affiliations.

Correspondence to: Stanley Liu, PhD, MD, FRCPC, Sunnybrook Health Sciences Centre, 2075 Bayview Avenue, Rm T2-142, Toronto, ON M4N 3M5, Canada (e-mail: Stanley.Liu@sunnybrook.ca) and Bharati Bapat, PhD, Lunenfeld-Tannenbaum Research Institute, 60 Murray Street, Rm L6-304B, Toronto, ON M5T 3L9, Canada (e-mail: bapat@lunenfeld.ca) and Paul C. Boutros, PhD, University of California, Los Angeles, 12-109 CHS, 10833 Le Conte Avenue, Los Angeles, CA 90024 (e-mail: pboutros@mednet.ucla.edu).

Abstract

Background: The development of noninvasive tests for the early detection of aggressive prostate tumors is a major unmet clinical need. miRNAs are promising noninvasive biomarkers: they play essential roles in tumorigenesis, are stable under diverse analytical conditions, and can be detected in body fluids.

Methods: We measured the longitudinal stability of 673 miRNAs by collecting serial urine samples from 10 patients with localized prostate cancer. We then measured temporally stable miRNAs in an independent training cohort (n = 99) and created a biomarker predictive of Gleason grade using machine-learning techniques. Finally, we validated this biomarker in an independent validation cohort (n = 40).

Results: We found that each individual has a specific urine miRNA fingerprint. These fingerprints are temporally stable and associated with specific biological functions. We identified seven miRNAs that were stable over time within individual patients and integrated them with machine-learning techniques to create a novel biomarker for prostate cancer that overcomes interindividual variability. Our urine biomarker robustly identified high-risk patients and achieved similar accuracy as tissue-based prognostic markers (area under the receiver operating characteristic = 0.72, 95% confidence interval = 0.69 to 0.76 in the training cohort, and area under the receiver operating characteristic curve = 0.74, 95% confidence interval = 0.55 to 0.92 in the validation cohort).

Conclusions: These data highlight the importance of quantifying intra- and intertumoral heterogeneity in biomarker development. This noninvasive biomarker may usefully supplement invasive or expensive radiologic- and tissue-based assays.

Prostate cancer is the most common nonskin male malignancy and the second-leading cause of oncological mortality for men in developed countries (1). Many prostate cancers are indolent at diagnosis (2). Clinical estimation of prostate cancer aggressivity uses serum prostate-specific antigen (PSA) measurement, digital rectal examination (DRE), and multiple prostate biopsies to assess tumor grade (Gleason Score [GS]) (3). The low specificity of the PSA test, low sensitivity of DREs, and complications of biopsies create an urgent clinical need for improved risk stratification (4). Further, the spatial-temporal genomic heterogeneity of prostate cancer (5,6) can confound tissue-based prognostic assays.

Received: April 5, 2018; **Revised:** March 1, 2019; **Accepted:** May 30, 2019

As a result, several noninvasive molecular tests for aggressive prostate cancer have been developed. Both increased cell-free DNA in plasma (7) and increased circulating tumor cells are associated with worse survival (8). Although these tests provide information on cancer detection and progression, their accurate and routine isolation and quantification remain technically challenging, particularly in curable prostate cancer that has not metastasized. Similarly, urine proteins are promising candidate biomarkers (9), but paths to clinical translation of mass-spectrometry assays remain unclear.

We therefore considered an alternate approach: urinary microRNAs (miRNAs). These small RNAs are involved in prostate cancer development and progression (10), influence treatment response (11), are stable under harsh conditions (eg, low and high pH) (12), and are detectable in urine (13). Urinary miRNAs therefore make good candidates as noninvasive biomarkers for prostate cancer, and their potential diagnostic and prognostic applications have been proposed (14,15). However, results from previous studies are limited by the small number of assayed miRNAs and the lack of sequential validations. Furthermore, inter- and intraindividual variations in miRNA transcriptome remain unclear because of the absence of repeated measurements of miRNA abundances for the same individual.

Here, we created the first cohorts of urine miRNA transcriptome profile linked to rich clinical data, quantified the longitudinal stability of miRNA profiles over multiple years, and showed that urinary miRNAs reflect primary tumor miRNA abundances. These data were used to create and validate an accurate urine biomarker of aggressive prostate cancer.

Methods

Urinary miRNA Extraction and Profiling

To quantify the intraindividual stability of urine miRNA transcriptome and examine its effect on cancer aggressivity, urine miRNA profiles of prostate cancer patients (n = 149) were generated. Small RNA molecules (200 nucleotides or less, including miRNAs) were isolated from urinary cell sediments using the Urine miRNA Purification kit (Norgen Biotek Corp., Thorold, Ontario, Canada, catalogue No. 29000) according to the manufacturer's protocol. Following isolation, RNA was purified using ammonium acetate-ethanol precipitation. Then, 25 μL of 7.5 mM ammonium acetate and 125 μL of cold 100% ethanol were added to isolated RNA samples (50 μL) and left at −80°C overnight. Next, 1 mL of cold 80% ethanol was added, and samples were centrifuged at 18 000 × g for 30 minutes at 4°C. RNA pellet was washed twice with 0.5 mL of cold 80% ethanol and centrifuged at 18 000 × g for 10 minutes at 4°C. Ethanol was removed, and pellets were allowed to dry at room temperature. Dried pellets were resuspended in 22 μL of nuclease-free water. The quality and quantity of RNA samples were evaluated using a NanoDrop 8000 Spectrophotometer (Thermo Scientific, Wilmington, DE). miRNA profiling was performed using nCounter Human v.2 miRNA Expression Assay (NanoString Technologies, Seattle, WA).

Urine miRNA profiles of 149 patients were generated from three patient cohorts. The discovery cohort was composed of 10 patients and used to measure intra- and interindividual variability of individual miRNA abundance and select intrastable miRNAs. The training cohort (n = 99) was composed of 50 high-risk (GS > 7) and 49 low-risk patients (GS = 6). It was used to build a predictive model to identify aggressive prostate cancer. Intrastable miRNAs were used as features to build the model. The validation cohort, which was composed of 11 high-risk and 29 low-risk patients, was used for further evaluation of prediction performance of the model. miRNA abundances of three cohorts were separately quantified using NanoString nCounter technology and normalized using NanoStringNorm (16) (v1.1.20; Supplementary Methods, available online). Raw data are deposited into the Gene Expression Omnibus (GSE86474, http://www.ncbi.nlm.nih.gov/geo/).

Quantify Intra- and Interindividual Variance of miRNA Abundance

The relative effects of intra- and interindividual miRNA variance were assessed via linear mixed-effects regression using the lme4 package (v1.1–10) in R statistical environment (17). In the model, subjects were specified as a random factor to control for their associated intraclass correlation,

$$Y_{ij} = \mu + A_j + e, \quad [1]$$

where Y is normalized abundance for the i^{th} replicate (sample) in the j^{th} individual (patient); μ is mean abundance for any miRNA (fixed effect). The individual (A) effect is assumed to be random with variance (random effect), and e is an unknown vector of random errors. To measure the intra- and interindividual variances, we calculated the intraclass correlation coefficient (ICC):

$$\mathrm{ICC} = \frac{\sigma_A^2}{\sigma_A^2 + \sigma_e^2}. \quad [2]$$

The ICC represents the proportion of interindividual variance relative to total intra- and interindividual variance explained by a model. A high ICC indicates a high level of interindividual variability relative to intraindividual variability. To measure ICCs of miRNAs, the discovery cohort was used (Supplementary Methods, available online).

Statistical Analysis

All analyses were carried out in the programming language R (v3.4.0) with the aforementioned packages. In general, unpaired two-sided Student t tests with Welch's adjustment for heteroscedasticity and the two-sided Wilcoxon test were used to examine statistical significance for two-group comparisons. To examine whether correlation between urine and tumor miRNA abundance was increased with intraindividual stability (Q100 > Q75 > Q50 > Q25), a one-tailed asymptotic general independence test was used. A P value of less than .05 was considered statistically significant. To evaluate the enriched chromo-somal position of intrastable and intravariable miRNAs, a bootstrap test with 10 000 iterations was used. To examine functional enrichment of intravariable and intrastable miRNAs, Benjamini-Hochberg–adjusted P values were used to account for multiple testing. Hierarchical clustering analysis was performed with the ConsensusClusterPlus package (v1.40.0) (18). Intrastable miRNAs (fourth quartile of ICCs; Q100) from the discovery cohort were used as a set of features. These miRNAs were selected from the training cohort to build a predictive model, with feature selection and predictor generation done using a random forest. Finally, the generated predictive model was applied to the independent validation cohort to evaluate the reliability of prediction

ARTICLE

performance, with the area under the receiver operating characteristic curve (or AUC) used as a metric of accuracy (Supplementary Methods, available online).

Results

miRNA Landscape of Prostate Cancer Urine

To generate robust biomarkers, it is critical that analyte profiles remain stable over time and distinctive between individuals. We employed NanoString nCounter technology to profile the abundances of 673 human miRNAs in 22 serial DRE-urine samples from 10 patients with localized prostate cancer (discovery cohort, two to three urine samples were collected from each patient; Figure 1A). These patients were monitored for disease progression without therapeutic intervention (ie, active surveillance) and were clinically homogeneous, with the same tumor grade (Gleason grade = 3+3, GS = 6) and disease extent (T1c; Supplementary Table 1, available online). The median time between urine collections was 245 days. We systematically assessed a panel of 252 preprocessing strategies (Figure 1B; Supplementary Methods, available online). The optimal strategy maximized control sample similarity (Spearman $\rho = 0.73$) and minimized the number of misinterpreted samples (Supplementary Figure 1A, available online), yielding similar distributions of miRNA abundances across all samples (Supplementary Figure 1B, available online).

Intra- and Interindividual Urinary miRNA Variability

A majority of assayed miRNAs were detected in urine: 71.5% (481 of 673) were present in at least one sample, 26.2% (176 of 673) in half, and 3.7% (25 of 673) in all 22 samples (Supplementary Figure 1C, available online). miRNAs detected in urine overlapped strongly with those expressed in prostate tumors (19): 80% of miRNAs detected in at least one urine sample were also detected in the low-risk samples (GS = 6) of the Cancer Genome Atlas primary tumors (Supplementary Figure 2, A and B, available online). Urinary miRNA abundance was directly correlated to tumor miRNA abundance (Spearman $\rho = 0.22$, $P < .001$; Supplementary Figure 2C, available online). There were 140 miRNAs observed in prostate tumors but not in urine (tissue-specific miRNAs; Supplementary Figure 2B, available online), which is approximately 5% more than expected by chance alone ($P < .001$, hypergeometric test), suggesting a bias in which miRNAs are shed into urine. Tissue-specific miRNAs had fewer targets (median: 2 genes) than miRNAs detected in urine (median: 6 genes, $P = .004$, two-sided Wilcoxon test; Supplementary Figure 2D, available online). It suggests that tissue-specific miRNAs would have less functional impact on downstream biological behaviors and therefore may be less relevant for biomarker discovery.

We focused analyses of longitudinal stability of urine miRNA profiles on the 298 miRNAs detected in at least five samples from the discovery cohort (Figure 1C; Supplementary Table 2, available online). Urinary miRNA abundance profiles were more similar within individuals ($\rho_{intra} = 0.67 \pm 0.10$) than between individuals ($\rho_{inter} = 0.40 \pm 0.15$, $P < .001$, two-sided Wilcoxon test; Figure 2A). Further, the primary difference within individuals is the numbers of miRNAs detected, rather than abundance changes within or between the set detected (Supplementary Figure 3, A and B, available online), suggesting differences in experimental sensitivity, not biology. Unsupervised k-means clustering confirmed that samples from the same individual group together (Supplementary Figure 4, A and B, available online).

To understand which miRNAs are most and least variable within individuals, we examined the intra- and interindividual coefficient of variation (Supplementary Figure 5, available online). Overall, 89.9% of miRNA species showed more variability between individuals than within individuals (Figure 2B). Next, to quantify the relative importance of intra- and interindividual variability for each miRNA, we performed linear mixed-effects modeling and measured the ICCs. The higher a miRNA's ICC, the more it varies across individuals. Overall, 40.8 (27.7%) of total variance occurs between individuals (Figure 2C), suggesting that a set of miRNAs show high variability within individuals. Thus, we identified urinary miRNAs that potentially could be excluded from biomarker-discovery studies, although this will need additional validation in additional cohorts (Supplementary Table 3, available online).

The Biological Consequences of miRNA Variability

It has been shown that human miRNAs cluster together along the genome and form stable secondary structures (20,21), and each miRNA cluster controls distinct cellular processes (22). To investigate the spatial variability of miRNAs, we created four quartiles of miRNAs based on their ICCs (Supplementary Figure 6A, available online). Those miRNAs most variable within individuals are in the first quartile (Q25, intravariable), whereas those least variable within individuals are in the fourth quartile (Q100, intrastable). Each quartile group is biased toward specific chromosomal locations (Figure 3A; Supplementary Figure 6B, available online). For example, intrastable miRNAs (Q100) are enriched on chromosomes 6 and 17 (both $q = 0.02$, bootstrap test). Overall, 60.0% of miRNAs on chromosome 6 and 47.1% of those on chromosome 17 are intrastable. Supporting the clinical relevance of intraindividual stability in profiles, intrastable miRNAs (Q100) were preferentially localized to regions shown to be copy-number neutral in a large cohort of primary prostate cancer (23) (Supplementary Figure 6C, available online).

These associations of variation and chromosomal location suggested that miRNAs that are intraindividually variable may play distinct biological roles by targeting a different set of genes. Using experimentally validated miRNA target genes (Supplementary Table 4, available online), we found that intrastable miRNAs (Q100) targeted more genes (median: 14 genes) than intravariable miRNAs (Q25, median: 4 genes, $P = .04$, two-sided Wilcoxon test; Figure 3B). Also, 67.9% of target genes (1133 of 1669 target genes, 122 + 185 + 307 + 519) were regulated by specific variable groups (Figure 3C). Indeed, miRNA variability was associated with the biological functions played by their target genes (Figure 3D; Supplementary Table 5, available online). For example, targets of intravariable miRNAs (Q25) are involved in the initiation or perpetuation of immune responses, whereas intrastable miRNAs (Q100) preferentially targeted genes located on the plasma membrane and involved in the organization of extracellular structure ($q < 0.05$).

Finally, we evaluated the association between urine and tumor tissue miRNA abundances using 480 tumors from the Cancer Genome Atlas. Intrastable miRNAs (Q100) showed the strongest correlation between urine and tumor miRNA abundance (Spearman $\rho = 0.45$, $P < .001$; Supplementary Figure 7A, available online), and the correlation increased with intraindividual stability (Q100 > Q75 > Q50 > Q25, asymptotic general independence test, one-tailed, $P = .04$; Supplementary Figure 7B, available online). Thus, intrastable urinary miRNAs appear to serve as partial surrogates for tumor miRNA abundances.

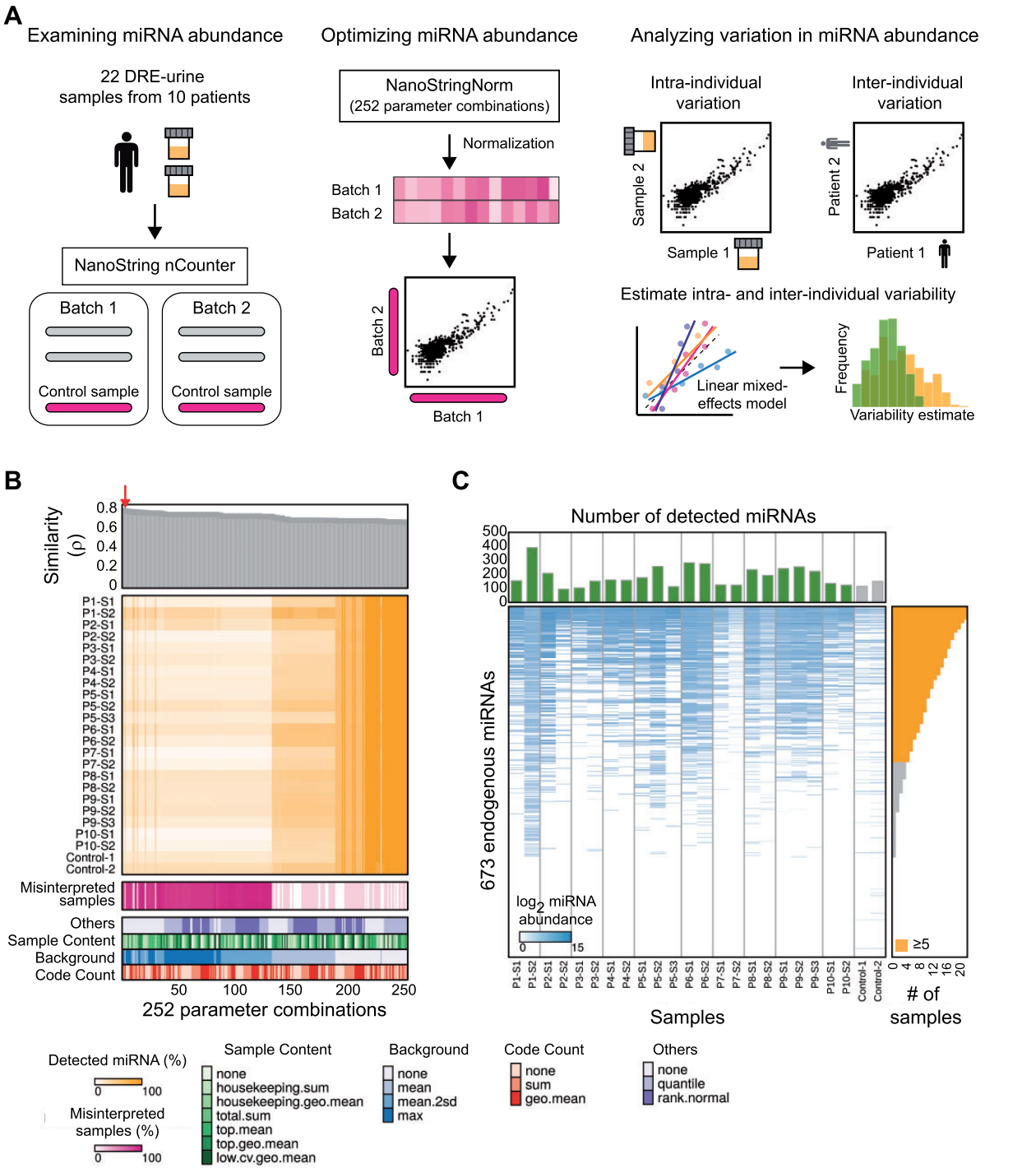

Figure 1. Digital rectal examination (DRE)-urine microRNA (miRNA) transcriptome profile. **A)** Overview of analysis of urine miRNA abundance variance in 10 prostate cancer patients. **B)** Parameter selection to optimize miRNA abundance. NanoString nCounter technology was used for miRNA abundance profiling. Similarity (ρ) represents miRNA profile similarity between two control samples. Misinterpreted samples indicate the fraction of samples with failed normalization. The similarity between control samples is likely to be increased when there are more misinterpreted samples. Because samples are misinterpreted when less than 10% of assayed miRNAs are detected after normalization, this correlation could be an inevitable effect of small size of detected miRNAs to calculate a similarity. To mitigate this effect, we only considered parameters that show high similarity between controls and zero misinterpreted samples (**arrow**). **C)** Normalized miRNA transcriptome profile. **Bars (top)** represent the number of detected miRNAs in patient urine and control samples, respectively. **Bars (right)** represent the number of samples a given miRNA is detected in (normalized transcript count > 0).

Urinary miRNAs Associated With Aggressive Prostate Cancer

Given that intrastable urinary miRNAs regulate distinct functional processes and reflect tumor miRNA abundances, we hypothesized that intrastable miRNAs could serve as noninvasive biomarkers for patient stratification into high- and low-risk groups. High-risk tumors are the most aggressive, and low-risk prostate tumors are unlikely to grow or spread for years

ARTICLE

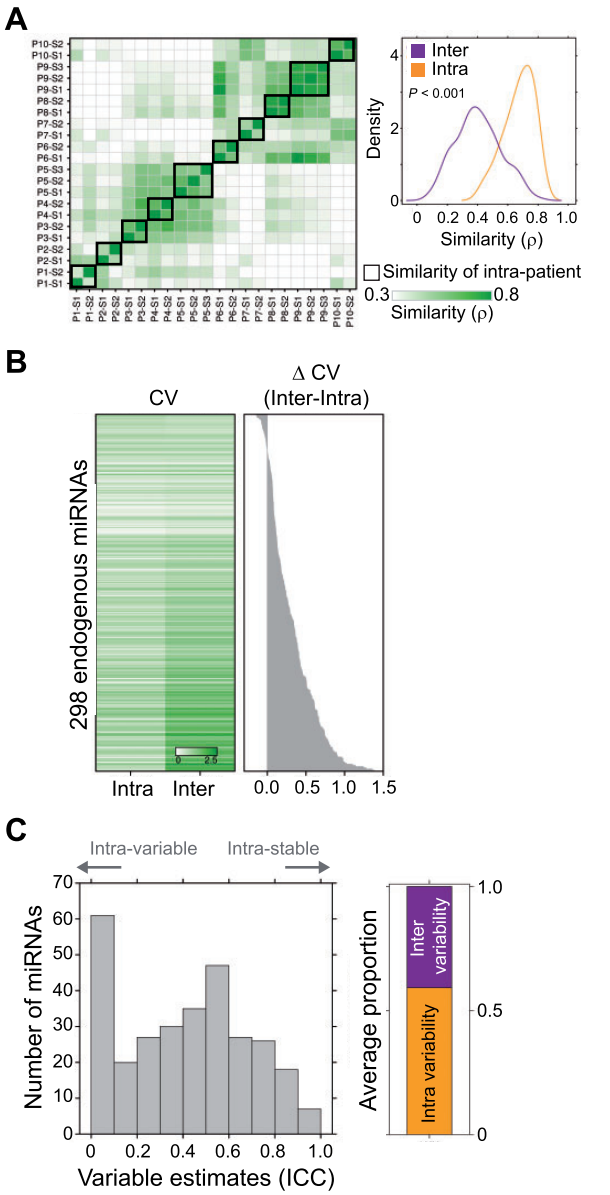

Figure 2. Intra- and interindividual variance of miRNA abundance. **A**) Global similarity of miRNA transcriptome. Distribution of correlation coefficient (ρ) of intra- and interindividual patients were compared using two-sided Wilcoxon test. **B**) Coefficient of variations (CVs) of 298 microRNAs (miRNAs) (**left**) and their differences between intra- and interindividual (**right**). **C**) The distribution of estimated variability of 298 miRNA abundances. Intra- and intervariability are estimated using intraclass correlation coefficient (ICC). Bar graph (**right**) shows the average proportion of intraindividual variability and interindividual variability of miRNA abundance.

(24). We examined the abundances of urinary miRNAs in an independent training cohort of 50 high-risk (GS > 7) and 49 low-risk (GS = 6) prostate tumors (Supplementary Figure 8A, available online). We identified six miRNAs differentially abundant between high- and low-risk prostate tumors (local false discovery rate < 0.2; Supplementary Figure 8B, available online). Five of these were in the third and fourth quartiles (Q75 and Q100). Indeed, miRNAs that are better at discriminating between risk groups are more likely to be stable within individuals (Supplementary Figure 8C, available online). These trends were also confirmed in primary tumor tissue (Supplementary Figure 8, D and E, available online).

Generation of a Urine miRNA Signature of Tumor Grade

Finally, we evaluated the ability of urinary miRNAs to distinguish aggressive disease progression (high-risk patients) from less-aggressive disease progression (low-risk patients). We used a standard biomarker generation strategy to create a multi-miRNA risk model: selecting intrastable miRNAs from the 10-patient discovery cohort, training a model in the 99-patient training cohort, and validating it in a third, independent 40-patient validation cohort (Figure 4A; Supplementary Table 6, available online). For feature selection, we performed fivefold cross-validation 10 times in the training cohort and measured miRNA importance. The top-ranked miRNAs were used to build a random forest model, with hyperparameter optimization in the training cohort (Supplementary Figure 9A and Supplementary Methods, available online). The final model comprised seven intrastable miRNAs (miR-3195, let-7b-5p, miR-144-3p, miR-451a, miR-148a-3p, miR-512-5p, and miR-431-5p; Supplementary Figure 9B, available online) and had a mean AUC of 0.72 in the training cohort (95% confidence interval = 0.69 to 0.76; Figure 4B). In the fully independent validation cohort (Supplementary Figure 10, available online), it distinguished risk groups with similar efficacy (AUC = 0.74, 95% confidence interval = 0.55 to 0.92; Figure 4C).

To quantify the importance of intraindividual temporal stability for biomarkers, we generated a signature from intravariable miRNAs (Q25), using the strategy outlined above. Not exploiting intrastable miRNA reduced prediction accuracy from an AUC of 0.74 to only 0.55 (Figure 4C). To evaluate the null distribution of urine miRNA biomarkers (25), we generated 10 000 random seven-miRNA sets and built a model from each. These random models had AUCs of 0.55 (0.07) (Figure 4C), statistically significantly lower than our seven-miRNA model (bootstrap $P = .003$, Figure 4D). Indeed, the point-estimate for the seven-miRNA model statistically significantly exceeded the accuracy of the majority of random models.

Finally, to verify whether these urine miRNAs accurately reflect miRNA abundances in tumor tissue, we profiled tumor tissue miRNAs from nine patients with matched urine samples (two high-risk and seven low-risk patients). The global abundance profiles across all 673 assayed miRNAs were positively correlated between matched urine and tumor (Spearman $\rho = 0.55$, $P < .001$; Supplementary Figure 11A, available online). To confirm the potential tumor origins of our biomarker, we examined the abundances of its seven component miRNAs. They were very strongly positively correlated (Spearman $\rho = 0.96$, $P = .003$; Supplementary Figure 11B, available online). Furthermore, urine miRNA abundances were positively correlated across discovery, training, and validation cohorts (Supplementary Figure 12, available online). These data indicate that intraindividual stability measured from the discovery cohort may represent general longitudinal stability and may support the ability of urine miRNA profiles to serve as surrogates for prostate tumor molecular and risk features, potentially by serving as a fluid sampling of it.

Discussion

Alterations in miRNA abundances are associated with prostate cancer progression (10), and these molecules can be detected in patient urine. miRNA abundances in urine are correlated to those of matched tumor tissues, implying that

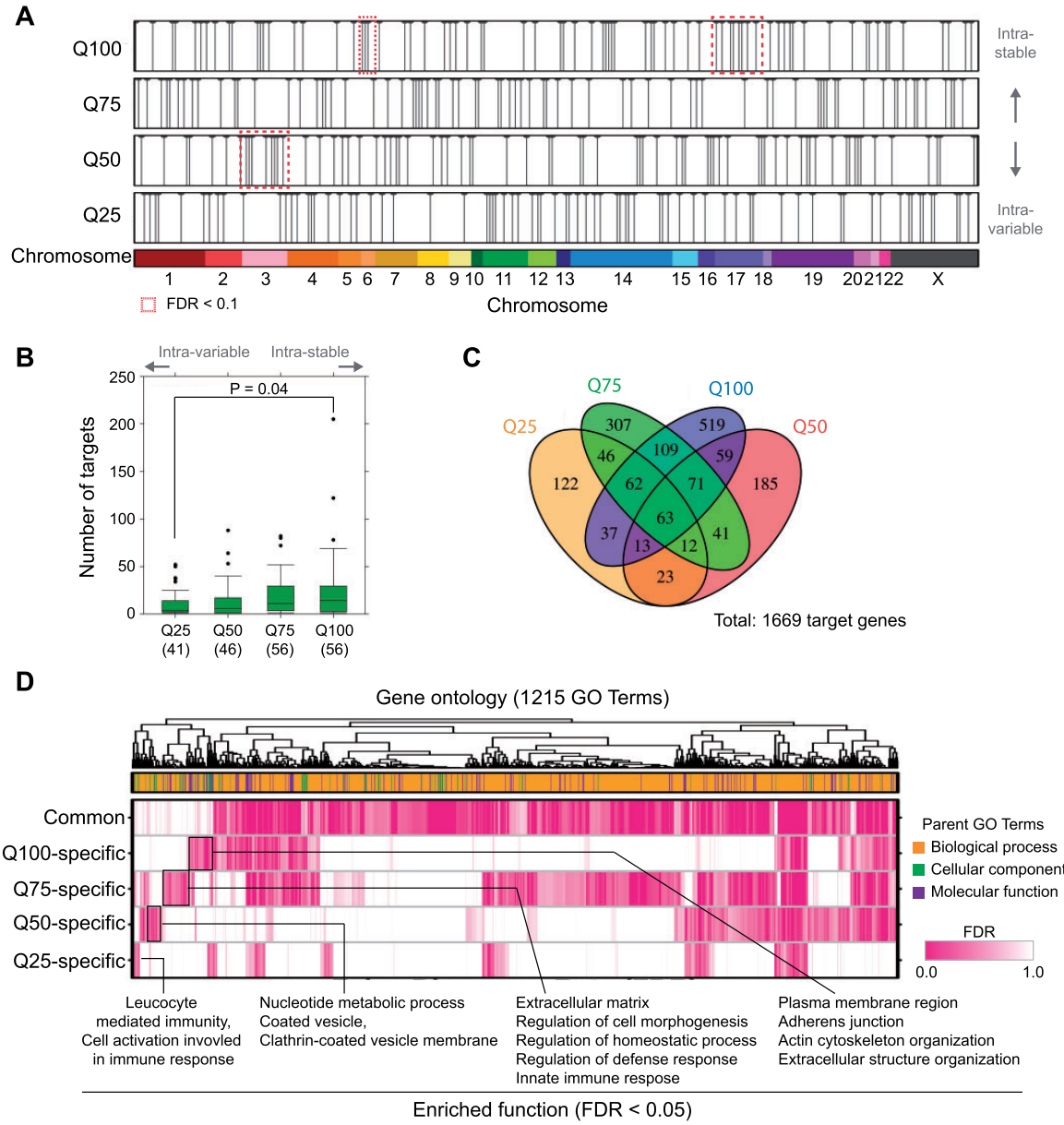

Figure 3. Biological properties of microRNAs (miRNAs) and their target genes. **A**) Chromosomal positions of assayed miRNAs. miRNAs are divided into four variable groups depending on intraclass correlation coefficient (ICC) (Q25, Q50, Q75, and Q100). **Dashed red boxes** indicate enriched chromosomes in a given variable group ($q < 0.1$). Q25 and Q100 represent miRNAs that are most and least variable within individuals, respectively. **B**) Number of target genes in variable groups. The number in parentheses under each variable group represents the total number of miRNAs that have known target genes. Two-sided Wilcoxon test was used to measure the statistically significant difference of the number of target genes of intrastable (Q100) and intravariable (Q25) miRNAs. **C**) Overlapped target genes among variable groups. **D**) Enriched biological functions of target genes in variable groups. In total, 1215 gene ontology (GO) terms showing $q < 0.25$ in at least one variable group are colored. Common indicates targets that are regulated by all four variable groups. Full GO terms and their enriched scores are in Supplementary Table 5 (available online). FDR = false discovery rate.

urine miRNA abundances may serve as a surrogate "liquid biopsy" of tumor miRNA abundances. Because the urine miRNA profile of an individual remains stable over longitudinal sampling taken more than a year apart, this suggests a biomarker-development strategy where individual miRNAs are evaluated based on both their temporal intraindividual stability and their degree of surrogacy. These stable and tumor-representative features would then be strong candidate features for biomarker development.

Nevertheless, intraindividual variability is observed and likely results at least in part from differences in the number of miRNAs detected, diet, polypharmacy and comorbid states, and other epidemiological factors. Recent studies of the placental mRNA transcriptome have shown similar intraindividual variance (26), as have tissue studies of mRNA and methylation (27, 28).

There are a few urine-based tests available for prostate cancer. Transcript levels of TDRD1, DLX1, and HOXC6 in DRE-urine (29) and those of ERG and PCA3 in urinary exosomes (30) have been used to identify high-grade prostate cancer (GS $\geq$ 7). Combined use of serum PSA level and transcript abundances of PCA3 and TMPRSS2-ERG in DRE-urine has shown diagnostic and prognostic value in the prediction of prostate cancer outcome

ARTICLE

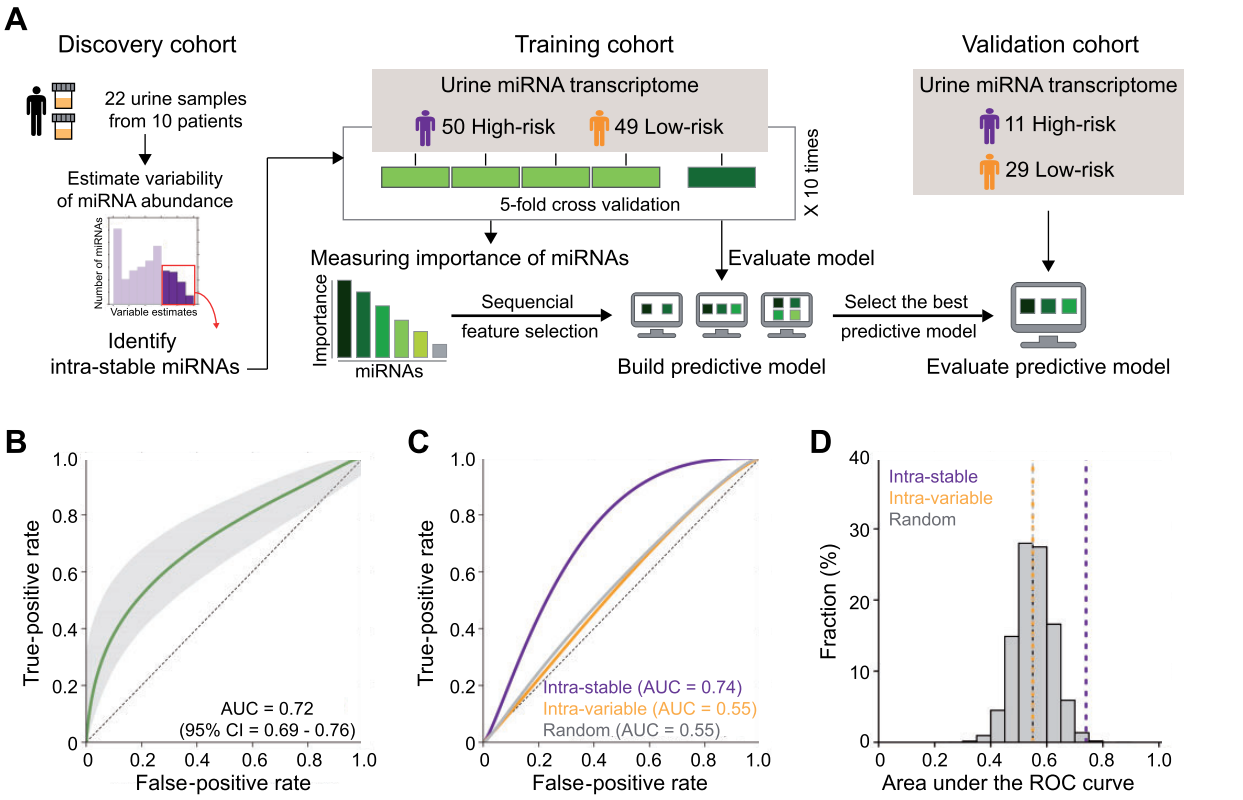

Figure 4. A predictive model distinguishes prostate cancer risk groups. **A)** Design of the machine-learning–based predictive model to classify two risk groups (high- and low-risk). **B)** The performance of predictive model in a training cohort (n = 99). **Bold line** indicates mean AUC of 10 times repeated fivefold cross-validation. **Shadow** indicates all cross-validated AUCs. **C)** The performance of predictive model in a validation cohort (n = 40). Receiver operating characteristic (ROC) curves of intrastable, intravariable, and randomly selected microRNA (miRNA) signatures are compared. **D)** AUC distribution of random models. In total, 10 000 random models were generated and their AUCs calculated. **Dashed vertical lines** represent AUCs of intrastable, intravariable, and randomly selected miRNA signatures (median AUC of random models). The intrastable signature has performance exceeding most randomly generated models. CI = confidence interval.

(31). However, these tests fail to correctly predict negative and low-grade prostate biopsies (30, 32), and discrepancies between the results of predictive models have been observed (33–36). Other studies using miRNAs have reported that miRNA levels in urine aid in the diagnosis (14, 37) and recurrence assessment of prostate cancer (15), yet these studies were not validated in independent patient cohorts.

We have provided a new strategy to generate a robust noninvasive miRNA biomarker using sequential validation of urinary miRNAs. Discovery cohort was generated from repeated urine samplings, allowing us to quantify abundance variances of miRNAs within an individual patient and identify intrastable miRNAs. Using an independent patient cohort, intrastable miRNAs were trained to develop a risk model that can predict the aggressivity of prostate cancer. Our model was further tested on a third validation cohort, achieving an AUC of 0.74, which is comparable to most tissue-based prognostic assays (38). This strategy improves both accuracy and generalizability of our risk model, and these benefits were realized from analysis of only 10 patients. Use of additional patients may refine the assessment of temporal stability for individual molecules and further improve biomarker discovery. To our knowledge, this is the first example of using intrastable urinary miRNAs as a biomarker of grade (which is itself a strong predictor for clinical outcome) in prostate cancer.

Encouragingly, the seven intrastable miRNAs used by our risk model are functionally associated with cancer aggressivity. For example, miR-451a and miR-148a have been implicated in the functional regulation of cell proliferation, migration, and invasion in prostate cancer (39, 40). Also, it has been shown that the deregulation of let-7b is associated with biochemical relapse in high-risk prostate cancer patients (41). miR-144-3p has been reported as a potential biomarker in colorectal cancer (42), and altered expressions of miR-3195 and miR-512-5p are associated with angiogenesis (43) and cell cycle (44) responses in cancer cell lines. Furthermore, we found that target genes of our miRNA biomarkers are enriched in cancer-related pathways such as PI3K-Akt (45), Jak-STAT (46), mTOR (47), and TGF-beta (48) signaling pathways as well as cell cycle (Supplementary Table 7, available online). Taken together, our seven-miRNA biomarker, comprised of molecules with temporally stable abundances, may help predict cancer aggressivity. The critical next step will be validation in larger patient cohorts.

There remains an urgent clinical need for accurate noninvasive tests of prostate cancer aggressiveness in both pre- and posttreatment settings. Prior to treatment, there is a need to avoid the discomfort, expenses, and complications of biopsies, which can include infection and sepsis (49). After treatment, rapid and accurate monitoring of disease relapse is needed, allowing for rapid adaptive treatment plans. Clinicopathological features such as PSA doubling time (50, 51) and percent of biopsy cores positive for cancer (52, 53) can stratify cancer patients with differential clinical outcomes. Similarly, age is correlated to prostate cancer-specific mortality for intermediate-risk patients (54). Urine miRNAs appear to serve as partial surrogates for

tumor miRNA abundances, therefore, integration of urine-derived signatures with clinic-pathological variables may improve prediction accuracy. One limitation of our study is that further validation of urine miRNA biomarkers in large tightly defined patient populations is required to improve risk stratification protocols for prostate cancer and perhaps other genitourinary diseases.

Funding

This study was conducted with the support of the Ontario Institute for Cancer Research to PCB through funding provided by the government of Ontario. PCB was supported by a Terry Fox Research Institute New Investigator Award and a Canadian Institutes of Health Research New Investigator Award. This work was awarded by Prostate Cancer Canada and is proudly funded by the Movember Foundation (grants RS2014-01 to PCB, TAG2014-01 to BB, and RS2014-03 to SL). SL is supported by an Ontario Ministry of Research and Innovation Early Researcher Award (ER14-10–035). This work was also supported by the Canadian Cancer Society, Relay for Life (Odette Cancer Centre), and Prostate Cancer Fight Foundation, Huronia Chapter of the Motorcycle Ride for Dad to SL and DV. This work was supported by the National Institutes of Health, National Cancer Institute under award number P30CA016042 and by an operating grant from the National Cancer Institute Early Detection Research Network (1U01CA214194-01).

Notes

Affiliations of authors: Ontario Institute for Cancer Research, Toronto, ON, Canada (JJ, HX, CQY, JDW, MF, PCB); Lunenfeld-Tannenbaum Research Institute, Sinai Health System, Toronto, ON, Canada (EOM, FZ, CC, RJ, BB); Sunnybrook Research Institute and Department of Radiation Oncology, Sunnybrook-Odette Cancer Centre, Toronto, ON, Canada (SJ, SS, JR, KC, AL, MD, DV, SL); Princess Margaret Cancer Centre, University Health Network, Toronto, ON, Canada (NEF, RGB); Department of Medical Biophysics (RGB, SL, PCB) and Department of Laboratory Medicine and Pathobiology (BB) and Department of Pharmacology & Toxicology (PCB), University of Toronto, Toronto, ON, Canada; Manchester Cancer Research Centre, University of Manchester, Manchester, UK (RGB); Department of Human Genetics (PCB) and Department of Urology (PCB) and Broad Stem Cell Research Centre (PCB) and Institute for Precision Health (PCB) and Jonsson Comprehensive Cancer Center (PCB), University of California, Los Angeles, Los Angeles, CA.

The funders had no role in the design of the study; the collection, analysis, and interpretation of the data; the writing of the manuscript; and the decision to submit the manuscript for publication.

The authors have no conflicts of interest to disclose.

Author contributions: Initiated the project: RGB, SL, BB, PCB. Generated tools and reagents: JJ, CQY, DV, SL, BB, PCB. Sample preparation: EOM, FZ, SJ, CC, SS, RJ, JDW, MF, JR, KC, AD, MD. Statistics and bioinformatics: JJ, HX, CQY, NEF, PCB. Supervised research: SL, BB, PCB. Wrote the first draft of the manuscript: JJ, PCB. Approved the manuscript: all authors.

We thank all members of the Boutros, Bapat, and Liu groups for advice and assistance.

References

1. Siegel R, Naishadham D, Jemal A. Cancer statistics, 2013. *CA Cancer J Clin*. 2013;63(1):11–30.
2. Musunuru HB, Yamamoto T, Klotz L, et al. Active surveillance for intermediate risk prostate cancer: survival outcomes in the Sunnybrook experience. *J Urol*. 2016;196(6):1651–1658.
3. Troyer DA, Mubiru J, Leach RJ, et al. Promise and challenge: markers of prostate cancer detection, diagnosis and prognosis. *Dis Markers*. 2004;20(2):117–128.
4. Loeb S, Vellekoop A, Ahmed HU, et al. Systematic review of complications of prostate biopsy. *Eur Urol*. 2013;64(6):876–892.
5. Cooper CS, Eeles R, Wedge DC, et al. Analysis of the genetic phylogeny of multifocal prostate cancer identifies multiple independent clonal expansions in neoplastic and morphologically normal prostate tissue. *Nat Genet*. 2015;47(4):367–372.
6. Boutros PC, Fraser M, Harding NJ, et al. Spatial genomic heterogeneity within localized, multifocal prostate cancer. *Nat Genet*. 2015;47(7):736–745.
7. Cortese R, Kwan A, Lalonde E, et al. Epigenetic markers of prostate cancer in plasma circulating DNA. *Hum Mol Genet*. 2012;21(16):3619–3631.
8. Danila DC, Heller G, Gignac GA, et al. Circulating tumor cell number and prognosis in progressive castration-resistant prostate cancer. *Clin Cancer Res*. 2007;13(23):7053–7058.
9. Kim Y, Jeon J, Mejia S, et al. Targeted proteomics identifies liquid-biopsy signatures for extracapsular prostate cancer. *Nat Commun*. 2016;7:11906.
10. Walter BA, Valera VA, Pinto PA, et al. Comprehensive microRNA profiling of prostate cancer. *J Cancer*. 2013;4(5):350–357.
11. Korpela E, Vesprini D, Liu SK. MicroRNA in radiotherapy: miRage or miRador? *Br J Cancer*. 2015;112(5):777–782.
12. Chen X, Ba Y, Ma L, et al. Characterization of microRNAs in serum: a novel class of biomarkers for diagnosis of cancer and other diseases. *Cell Res*. 2008;18(10):997–1006.
13. Korzeniewski N, Tosev G, Pahernik S, et al. Identification of cell-free microRNAs in the urine of patients with prostate cancer. *Urol Oncol*. 2015;33(1):16.e17–22.
14. Salido-Guadarrama AI, Morales-Montor JG, Rangel EC, et al. Urinary microRNA-based signature improves accuracy of detection of clinically relevant prostate cancer within the prostate-specific antigen grey zone. *Mol Med Rep*. 2016;13(6):4549–4560.
15. Fredsoe J, Rasmussen AKI, Thomsen AR, et al. Diagnostic and prognostic MicroRNA biomarkers for prostate cancer in cell-free urine. *Eur Urol Focus*. 2018;4(6):825–833.
16. Waggott D, Chu K, Yin S, et al. NanoStringNorm: an extensible R package for the pre-processing of NanoString mRNA and miRNA data. *Bioinformatics*. 2012;28(11):1546–1548.
17. Bates D, Maechler M, Bolker B, et al. Fitting linear mixed-effects models using lme4. *J Stat Softw*. 2015;67(1):1–48.
18. Wilkerson MD, Hayes DN. ConsensusClusterPlus: a class discovery tool with confidence assessments and item tracking. *Bioinformatics*. 2010;26(12):1572–1573.
19. Cancer GARN. The molecular taxonomy of primary prostate cancer. *Cell*. 2015;163(4):1011–1025.
20. Mathelier A, Carbone A. Large scale chromosomal mapping of human microRNA structural clusters. *Nucleic Acids Res*. 2013;41(8):4392–4408.
21. Kamanu TK, Radovanovic A, Archer JA, et al. Exploration of miRNA families for hypotheses generation. *Sci Rep*. 2013;3:2940.
22. Hausser J, Zavolan M. Identification and consequences of miRNA-target interactions—beyond repression of gene expression. *Nat Rev Genet*. 2014;15(9):599–612.
23. Fraser M, Sabelnykova VY, Yamaguchi TN, et al. Genomic hallmarks of localized, non-indolent prostate cancer. *Nature*. 2017;541(7637):359–364.
24. Carter HB. Management of low (favourable)-risk prostate cancer. *BJU Int*. 2011;108(11):1684–1695.
25. Boutros PC, Lau SK, Pintilie M, et al. Prognostic gene signatures for non-small-cell lung cancer. *Proc Natl Acad Sci USA*. 2009;106(8):2824–2828.
26. Hughes DA, Kircher M, He Z, et al. Evaluating intra- and inter-individual variation in the human placental transcriptome. *Genome Biol*. 2015;16;54.
27. Cowley MJ, Cotsapas CJ, Williams RB, et al. Intra- and inter-individual genetic differences in gene expression. *Mamm Genome*. 2009;20(5):281–295.
28. Turan N, Katari S, Gerson LF, et al. Inter- and intra-individual variation in allele-specific DNA methylation and gene expression in children conceived using assisted reproductive technology. *PLoS Genet*. 2010;6(7):e1001033.
29. Leyten GH, Hessels D, Smit FP, et al. Identification of a candidate gene panel for the early diagnosis of prostate cancer. *Clin Cancer Res*. 2015;21(13):3061–3070.
30. Donovan MJ, Noerholm M, Bentink S, et al. A molecular signature of PCA3 and ERG exosomal RNA from non-DRE urine is predictive of initial prostate biopsy result. *Prostate Cancer Prostatic Dis*. 2015;18(4):370–375.
31. Cornu JN, Cancel-Tassin G, Egrot C, et al. Urine TMPRSS2: ERG fusion transcript integrated with PCA3 score, genotyping, and biological features are correlated to the results of prostatic biopsies in men at risk of prostate cancer. *Prostate*. 2013;73(3):242–249.

ARTICLE

32. McKiernan J, Donovan MJ, O'Neill V, et al. A novel urine exosome gene expression assay to predict high-grade prostate cancer at initial biopsy. *JAMA Oncol*. 2016;2(7):882–889.
33. Hagen RM, Adamo P, Karamat S, et al. Quantitative analysis of ERG expression and its splice isoforms in formalin-fixed, paraffin-embedded prostate cancer samples: association with seminal vesicle invasion and biochemical recurrence. *Am J Clin Pathol*. 2014;142(4):533–540.
34. Robert G, Jannink S, Smit F, et al. Rational basis for the combination of PCA3 and TMPRSS2: ERG gene fusion for prostate cancer diagnosis. *Prostate*. 2013; 73(2):113–120.
35. Leyten GH, Hessels D, Jannink SA, et al. Prospective multicentre evaluation of PCA3 and TMPRSS2-ERG gene fusions as diagnostic and prognostic urinary biomarkers for prostate cancer. *Eur Urol*. 2014;65(3):534–542.
36. Tomlins SA, Aubin SM, Siddiqui J, et al. Urine TMPRSS2: ERG fusion transcript stratifies prostate cancer risk in men with elevated serum PSA. *Sci Transl Med*. 2011;3(94):94ra72.
37. Rodriguez M, Bajo-Santos C, Hessvik NP, et al. Identification of noninvasive miRNAs biomarkers for prostate cancer by deep sequencing analysis of urinary exosomes. *Mol Cancer*. 2017;16(1):156.
38. Lalonde E, Ishkanian AS, Sykes J, et al. Tumor genomic and microenvironmental heterogeneity for integrated prediction of 5-year biochemical recurrence of prostate cancer: a retrospective cohort study. *Lancet Oncol*. 2014; 15(13):1521–1532.
39. Chang C, Liu J, He W, et al. A regulatory circuit HP1gamma/miR-451a/c-Myc promotes prostate cancer progression. *Oncogene*. 2018;37(4):415–426.
40. Murata T, Takayama K, Katayama S, et al. miR-148a is an androgen-responsive microRNA that promotes LNCaP prostate cell growth by repressing its target CAND1 expression. *Prostate Cancer Prostatic Dis*. 2010;13(4): 356–361.
41. Schubert M, Spahn M, Kneitz S, et al. Distinct microRNA expression profile in prostate cancer patients with early clinical failure and the impact of let-7 as prognostic marker in high-risk prostate cancer. *PLoS One*. 2013;8(6): e65064.
42. Kalimutho M, Del Vecchio Blanco G, Di Cecilia S, et al. Differential expression of miR-144* as a novel fecal-based diagnostic marker for colorectal cancer. *J Gastroenterol*. 2011;46(12):1391–1402.
43. Sohn EJ, Won G, Lee J, et al. Upregulation of miRNA3195 and miRNA374b mediates the anti-angiogenic properties of melatonin in hypoxic PC-3 prostate cancer cells. *J Cancer*. 2015;6(1):19–28.
44. McCann MJ, Rotjanapun K, Hesketh JE, et al. Expression profiling indicating low selenium-sensitive microRNA levels linked to cell cycle and cell stress response pathways in the CaCo-2 cell line. *Br J Nutr*. 2017;117(9):1212–1221.
45. Shukla S, Maclennan GT, Hartman DJ, et al. Activation of PI3K-Akt signaling pathway promotes prostate cancer cell invasion. *Int J Cancer*. 2007;121(7): 1424–1432.
46. Liu X, He Z, Li CH, et al. Correlation analysis of JAK-STAT pathway components on prognosis of patients with prostate cancer. *Pathol Oncol Res*. 2012; 18(1):17–23.
47. Stelloo S, Sanders J, Nevedomskaya E, et al. mTOR pathway activation is a favorable prognostic factor in human prostate adenocarcinoma. *Oncotarget*. 2016;7(22):32916–32924.
48. Javle M, Li Y, Tan D, et al. Biomarkers of TGF-beta signaling pathway and prognosis of pancreatic cancer. *PLoS One*. 2014;9(1):e85942.
49. Djavan B, Waldert M, Zlotta A, et al. Safety and morbidity of first and repeat transrectal ultrasound guided prostate needle biopsies: results of a prospective European prostate cancer detection study. *J Urol*. 2001;166(3):856–860.
50. Klotz L. Active surveillance with selective delayed intervention using PSA doubling time for good risk prostate cancer. *Eur Urol*. 2005;47(1):16–21.
51. Freedland SJ, Humphreys EB, Mangold LA, et al. Risk of prostate cancer-specific mortality following biochemical recurrence after radical prostatectomy. *JAMA*. 2005;294(4):433–439.
52. Lotan Y, Shariat SF, Khoddami SM, et al. The percent of biopsy cores positive for cancer is a predictor of advanced pathological stage and poor clinical outcomes in patients treated with radical prostatectomy. *J Urol*. 2004;171(6 pt 1):2209–2214.
53. Spalding AC, Daignault S, Sandler HM, et al. Percent positive biopsy cores as a prognostic factor for prostate cancer treated with external beam radiation. *Urology*. 2007;69(5):936–940.
54. Arvold ND, Chen MH, Moul JW, et al. Risk of death from prostate cancer after radical prostatectomy or brachytherapy in men with low or intermediate risk disease. *J Urol*. 2011;186(1):91–96.